Materials Research. 2011; 14(2): 178-188
DOI: 10.1590/S1516-14392011005000030

The Effects of ZnO_2 Nanoparticles on Strength Assessments and Water Permeability of Concrete in Different Curing Media

Ali Nazari*, Shadi Riahi

Department of Materials Science and Engineering, Saveh Branch, Islamic Azad University, Saveh, Iran

Received: September 29, 2010; Revised: April, 13, 2011

In this study, the effect of limewater on strength assessments and percentage of water absorption of concrete incorporating ZnO_2 nanoparticles has been investigated. Portland cement was partially replaced by ZnO_2 nanoparticles with the average particle size of 15 nm and the specimens were cured in water and saturated limewater for specific ages. The results indicate that ZnO_2 nanoparticles up to 2.0 weight percent could produce concrete with improved strength and water permeability when the specimens cured in saturated limewater while this content is 1.0 weight percent for the specimens cured in tap water. Although the limewater reduces the strength of concrete without nanoparticles when compared with the specimens cured in water, curing the specimens bearing ZnO_2 nanoparticles in saturated limewater results in more strengthening gel formation around nanoparticles causes improved permeability together with high strength. In addition, ZnO_2 nanoparticles are able to act as nanofillers and recover the pore structure of the specimens by decreasing harmful pores. Accelerated peak appearance in conduction calorimetry tests, more weight loss in thermogravimetric analysis and more rapid appearance of peaks related to hydrated products in X-ray diffraction results, all indicate that ZnO_2 nanoparticles could improve mechanical and physical properties of the specimens.

Keywords: *ZnO_2 nanoparticle, compressive strength, split tensile strength, flexural strength, percentage of water absorption, curing medium, concrete, TGA, XRD, pore structure*

1. Introduction

Portland cement-based binders are the primary active components of concrete used in most modern construction. The other components are water and both fine and coarse aggregate. Binders are made from Portland "clinker" ground together with a little calcium sulfate, and frequently also contain fine mineral powders such as limestone, pozzolan (typically volcanic ash), fly ash (usually from coal-burning power plants) and granulated blast furnace slag. Such powders are referred to as supplementary cementitious materials (SCMs) since they are used to replace some of the more expensive clinker. Chemical admixtures such as superplasticisers and air-entraining agents can be added in small amounts to modify the properties of a concrete for specific applications. Because of ultrafine size, nanoparticles show unique physical and chemical properties different from those of the conventional materials. As a result of their unique properties, nanoparticles have been gained specific attention and been applied in many fields to fabricate new materials with novelty functions. If nanoparticles are integrated with traditional building materials, the new materials might possess outstanding or smart properties for the construction of super high-rise, long-span or intelligent civil infrastructure systems[1].

There are several reports on incorporation of nanoparticles in concrete specimens which most of them have focused on using SiO_2 nanoparticles[2-10] and TiO_2 nanoparticles[11,12]. There are a few studies on incorporating nano-Fe_2O_3[13], nano-Al_2O_3[14], and nanoclay particles[15,16]. Additionally, a limited number of investigations are dealing with the manufacture of nanosized cement particles and the development of nanobinders[17]. In our previous works[22-35], we tried to investigate the effects of different nanoparticles such as SiO_2[18-21], TiO_2[22-25], Al_2O_3[26,27], ZnO_2[28], ZrO_2[29-31], Fe_2O_3[32], Cr_2O_3[33,34] and CuO[35] nanoparticles on different concrete admixtures. In the all works[22-35], we found that nanoparticles can act as heterogeneous nuclei for cement pastes, further accelerating cement hydration because of their high reactivity, as nano-reinforcement, and as nano-filler, densifying the microstructure, thereby, leading to a reduced porosity. The most significant issue for all nanoparticles is that of effective dispersion.

The beneficial action of the nanoparticles on the microstructure and performance of cement-based materials can be explained by the following factors[36,37]:

- Nanoparticles fill the voids between cement grains, resulting in the immobilization of "free" water ("filler" effect);
- Well-dispersed nanoparticles act as centers of crystallization of cement hydrates, hence accelerating the hydration;
- Nanoparticles favor the formation of small-sized crystals (such as $Ca(OH)_2$ and AF_m) and small-sized uniform clusters of C-S-H;
- Nanoparticles contribute in the pozzolanic reactions or accelerate them, resulting in the consumption of $Ca(OH)_2$ and formation of an "additional" C-S-H gel;
- Nanoparticles improve the structure of the aggregates' contact zone, resulting in a better bond between aggregates and cement paste; and
- Nanoparticles provide crack arrest and interlocking effects between the slip planes, which improve the toughness, shear, tensile and flexural strength of cement-based materials.

Strength assessment of concrete is a main and probably the most important mechanical property, which is usually measured after a standard curing time. Concrete strength is influenced by lots of factors

*e-mail: alinazari84@aut.ac.ir

like concrete ingredients, age, ratio of water to cementitious materials, etc. The pore structure determines the transport properties of cement paste, such as permeability and ion migration. In the hydrated paste, the capillary and gel pores can be distinguished. The gel pores are very small. Although they constitute a network of open pores, the permeability of this network is very low. Conversely, the capillary pores are relatively large spaces existing between the cement grains. It is the capillary porosity that greatly affects the permeability of concrete[38]. Permeability of cement paste is a fundamental property in view of the durability of concrete: it represents the ease with which water or other fluids can move through concrete, thereby transporting aggressive agents. It is therefore of utmost importance to investigate the quantitative relationships between the pore structure and the permeability. Through experimental studies of the pore structure and the permeability of cement-based materials, a better understanding of transport phenomena and associated degradation mechanisms will hopefully be reached[39].

The aim of this study is to investigate mechanical properties and water permeability of concrete specimens containing different amount of ZnO_2 nanoparticles which are cured in different curing media. In addition, the effects of ZnO_2 nanoparticles on microstructure, pore structure and thermal properties have been investigated when the specimens cured in water or saturated limewater at different ages. Furthermore, some empirical relationships have been presented to correlate the compressive strength to flexural strength and split tensile strength of the specimens.

2. Materials and Methods

Ordinary Portland Cement (OPC) conforming to ASTM C150[40] standard was used as received. The chemical and physical properties of the cement are shown in Table 1. In addition, the distribution pattern of cement particles determined by BET method has been illustrated in the previous works[18-35].

Nano–ZnO_2 with average particle size of 15 nm producing from Suzhou Fuer Import&Export Trade Co., Ltd was used as received. The properties of nano- ZnO_2 particles are shown in Table 2. Scanning electron micrographs (SEM) and powder X-ray diffraction (XRD) diagrams of ZnO_2 nanoparticles have been shown in the previous works[28,29].

Locally available natural sand with particles smaller than 0.5 mm and fineness modulus of 2.25 and specific gravity of 2.58 $g.cm^{-3}$ (loose form) was used as fine aggregate. Crushed basalt stored in the laboratory with maximum size of 15 mm and specific gravity of 2.96 $g.cm^{-3}$ (loose form) was used as coarse aggregate.

Two series of mixtures were prepared in the laboratory trials. C0 Series mixtures were prepared as control specimens. The control mixtures were made of natural aggregates, cement and water. N series were prepared with different contents of nano- ZnO_2 particles with average particle size of 15 nm. The mixtures were prepared with the cement replacement of 0.5, 1.0, 1.5 and 2.0% by weight. The water to binder ratio for all mixtures was set at 0.40. The aggregates for the mixtures consisted of a combination of crushed basalt and of fine sand, with 30 wt. (%) of sand. The binder content of all mixtures was 450 $kg.m^{-3}$. The proportions of the mixtures are presented in Table 3.

N series mixtures were prepared by mixing the course aggregates, fine aggregates and powder materials (cement and nano- ZnO_2 particles) in a laboratory concrete drum mixer. The powder material in the C0 series mixtures was only cement. They were mixed in dry condition for two minutes, and for another three minutes after adding the water. Cubes of 100 mm edge for compressive strength tests, cubes with 200 × 50 × 50 mm edges for flexural strength and cylinders with the diameter of 150 mm and the height of 300 mm for split tensile strength were cast and compacted in two layers on a vibrating table, where each layer was vibrated for 10 seconds. The moulds were covered with polyethylene sheets and moistened for 24 hours. Then the specimens were demolded and cured in water (N-W series) and saturated limewater (N-LW series) at a temperature of 20 °C prior to test days. To produce saturated limewater, the lime powder was solved in tap water and dispersed until the excess lime powder was precipitated. The strength tests of the concrete samples were determined at 7, 28 and 90 days after curing. After each time of the curing, the old limewater media was renewed to maintain saturated limewater.

Compressive strength of nano- ZnO_2 particles blended cement concrete cubes was determined in accordance to the ASTM C 39[41] after 7, 28 and 90 days of moisture curing. Tests were carried out on triplicate specimens and average compressive strength values were considered.

Split tensile test was carried out in accordance to the ASTM C496[42] standard. After the specified curing period was over, the concrete cylinders were subjected to split tensile test by using universal testing machine. Tests were carried out on triplicate specimens and average split tensile strength values were obtained.

Flexural test were done in accordance to the ASTM C293[43] standard. Again, flexural tests were carried out on triplicate specimens and average flexural strength values were obtained.

Standard slump tests conforming to ASTM C143[44] were used to determine the workability of the concrete.

Water permeability tests are performed with several methods such as percentage of water absorption, rate of water absorption and coefficient of water absorption. In this work, to evaluate the water permeability of the specimens, percentage of water absorption is an evaluation of the pore volume or porosity of concrete after hardening, which is occupied by water in saturated state. Water absorption values of ZnO_2 nanoparticle blended concrete samples were measured as per ASTM C 642[45] after 7, 28 and 90 days of moisture curing.

Mercury intrusion porosimetry (MIP) is extensively used to characterize the pore structure in porous material as a result of its simplicity, quickness and wide measuring range of pore diameter[46,47]. MIP provides information about the connectivity of pores[46]. In this study, the pore structure of concrete is evaluated by using MIP. To prepare the samples for MIP measurement, the concrete specimens after 90 days of curing are first broken into smaller pieces, and then the cement paste fragments selected from the center of prisms are used to measure pore structure. The samples are immersed in acetone to stop hydration as fast as possible. Before mercury intrusion test, the samples are dried in an oven at about 110 °C until constant weight to remove moisture in the pores. MIP is based on the assumption that the non-wetting liquid mercury (the contact angle between mercury and solid is greater than 90°) will only intrude in the pores of porous material under pressure[46,47]. Each pore size is quantitatively determined from the relationship between the volume of intruded mercury and the applied pressure[47]. The relationship between the pore diameter and applied pressure is generally described by Washburn equation as follows[46,47]:

$$D = -4\gamma\cos\theta / P \quad (1)$$

where, D is the pore diameter (nm), γ is the surface tension of mercury ($dyne.cm^{-1}$), θ is the contact angle between mercury and solid (°) and P is the applied pressure (MPa). The test apparatus used for pore structure measurement is Auto Pore III mercury porosimeter. Mercury density is 13.5335 $g.mL^{-1}$. The surface tension of mercury is taken as 485 $dynes.cm^{-1}$, and the contact angle selected is 130°. The maximum measuring pressure applied is 200 MPa (30000 psi), which

Table 1. Chemical and physical properties of Portland cement wt. (%).

Material	SiO_2	Al_2O_3	Fe_2O_3	CaO	MgO	SO_3	Na_2O	K_2O	Loss on ignition
Cement	21.89	5.3	3.34	53.27	6.45	3.67	0.18	0.98	3.21

Specific gravity: 1.7 $g.cm^{-3}$.

Table 2. The properties of nano- ZnO_2.

Diameter (nm)	Surface volume ratio ($m^2.g^{-1}$)	Density ($g.cm^{-3}$)	Purity (%)
15 ± 3	155 ± 12	<0.12	>99.9

Table 3. Mixture proportion of nano- ZnO_2 particles blended concretes.

Sample designation	Nano- ZnO_2 particles	Quantities, $kg.m^{-3}$	
		Cement	Nano- ZnO_2 particles
C0 (control)	0	450	0
N1	0.5	447.75	2.25
N2	1.0	445.50	4.50
N3	1.5	443.25	6.75
N4	2.0	441.00	9.00

Water to binder [cement + nano- ZnO_2] ratio of 0.40, sand 492 $kg.m^{-3}$, and aggregate 1148 $kg.m^{-3}$.

means that the smallest pore diameter that can be measured reaches about 6 nm (on the assumption that all pores have cylindrical shape).

Conduction calorimetry test was run out on a Wexham Developments JAF model isothermal calorimeter, using IBM program AWCAL-4, at 22 °C for a maximum of 70 hours. Fifteen grams of cement was mixed with water and saturated limewater and admixture before introducing it into the calorimeter cell.

A Netzsch model STA 409 simultaneous thermal analyzer equipped with a Data Acquisition System 414/1 programmer was used for thermogravimetric analysis. Specimens which were cured in water and saturated limewater for 90 days were heated from 110 to 650 °C, at a heating rate of 4 °C/min in an inert N_2 atmosphere.

SEM investigations were conducted on a Hitachi apparatus. Backscattered electron (BSE) and secondary electron (SE) imaging was used to study the samples, which were prepared under conditions that ensured their subsequent viability for analytical purposes.

A Philips PW-1730 unit was used for XRD analysis which was taken from 4 to 70°.

3. Results and Discussion

3.1. Compressive strength

The compressive strength results of C0-W and N-W series mixtures are shown in Figure 1. By comparison the compressive strength of the specimens cured for 7, 28 and 90 days, it could be observed that the compressive strength increases with nano- ZnO_2 particles up to 1.0% replacement (N2-W) and then it decreases, although the results of 2.0% replacement (N4-W) is still higher than those of the plain cement concrete (C0-W). It was shown that using 2.0% nano- ZnO_2 particles in N-W series decreases the compressive strength to a value which is near to the control concrete. This may be due to this fact that the quantity of nano- ZnO_2 particles present in the mix is higher than the amount required to combine with the liberated lime during the process of hydration thus leading to excess silica leaching out and causing a deficiency in strength as it replaces part of the cementitious material but does not contribute to strength[48]. Also, it may be due to the defects generated in dispersion of nanoparticles that causes weak zones. The high enhancement of compressive strength in the N series blended concrete are due to the rapid consuming of $Ca(OH)_2$ which was formed during hydration of Portland cement specially at early ages related to the high reactivity of nano- ZnO_2 particles. As a consequence, the hydration of cement is accelerated and larger volumes of reaction products are formed. Also nano- ZnO_2 particles recover the particle packing density of the blended cement, directing to a reduced volume of larger pores in the cement paste. Figures 2 and 3 respectively show the SEM micrograph of concrete without and with ZnO_2 nanoparticles after 7 days of curing in water. C–S–H gel which is existed in isolation is enclosed by some of needle-hydrates in the SEM micrograph of cement paste (Figure 2). On the other hand, the micrograph of the mixture containing nano- ZnO_2 revealed a compact formation of hydration products and a reduced content of $Ca(OH)_2$ crystals (Figure 3). In addition XRD results of the cement pastes with and without ZnO_2 nanoparticles after 15 hours of curing in water has been illustrated in Figure 4. The results show that after 15 hours of curing, $Ca(OH)_2$ crystals which needs to formation of C-S-H gel appears in concrete with ZnO_2 nanoparticles while for concrete without ZnO_2 nanoparticles it is not appeared indicating synergic effects of ZnO_2 nanoparticles on formation of subsequent C-S-H gel.

Figure 1 also shows the compressive strength of C0-LW and N-LW series. The results show that the replacement of cement by ZnO_2 nanoparticles up to 2.0 wt. (%) (N4-LW) in N-LW series produces concrete with high strength with respect to N-LW concrete. By comparison the compressive strength results of C0-W and C0-LW series, it shows that after 7, 28 and 90 days of curing the concrete in the saturated limewater, the compressive strength of the C0-LW series is smaller than the corresponding strength of C0-W series. This may be due to more formation of crystalline $Ca(OH)_2$ in the presence of limewater which reduces the compressive strength in C0-LW series with respect to C0-W series. On the other hand, the compressive strength of the N-LW series is more than those of N-W series. Lime reacts with water and produces $Ca(OH)_2$ which needs to form strengthening gel[49]:

$$CaO + H_2O = Ca(OH)_2 + Heat \quad (2)$$

When ZnO_2 nanoparticles react with $Ca(OH)_2$ produced from saturated limewater, the content of strengthening gel is increased because of high free energy of nanoparticles which reduces significantly when reacts by $Ca(OH)_2$[50]. The compressive strength of N-W and N-LW series should be compared from two viewpoints:

1. The compressive strength of N-LW series increases by partial replacement of cement with ZnO_2 nanoparticles up to 2.0 wt. (%) (N4-LW) while for N-W series it increases by partial replacement of cement with ZnO_2 nanoparticles up to 1.0 wt. (%) (N2-W) and then decreases. Once more this confirm the more strengthening gel formation in the presence of saturated limewater in which the quantity of nano- ZnO_2 particles present in the mix is close to the amount required to combine with the liberated lime during the process of hydration thus leading to lesser silica leaching out with respect to the specimens cured in water[50]; and

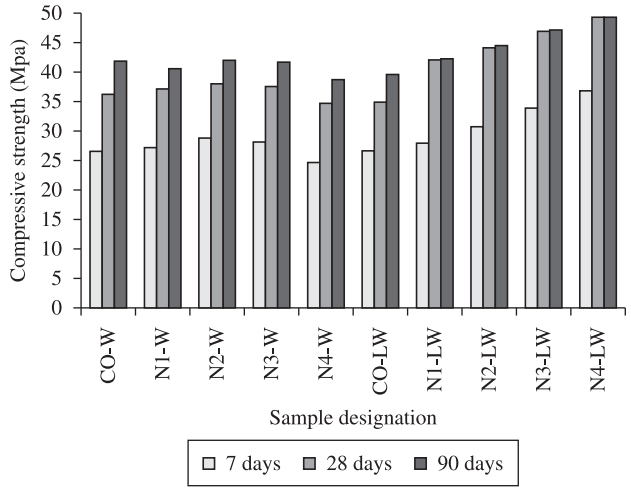

Figure 1. Compressive strength of nano- ZnO_2 particle blended concrete specimens.

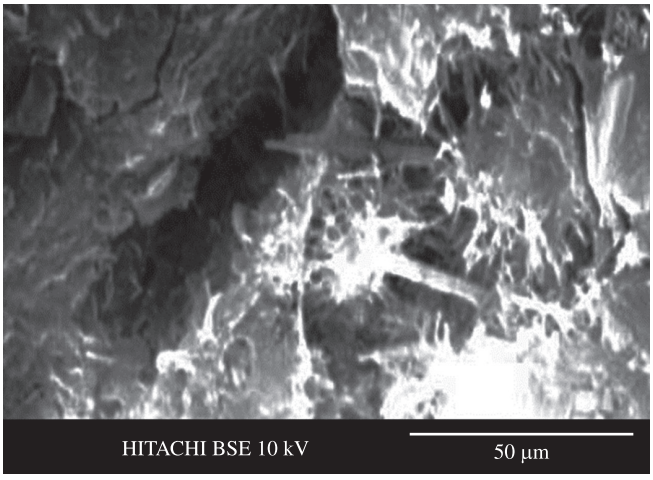

Figure 2. SEM micrograph of cement paste without ZnO_2 nanoparticles.

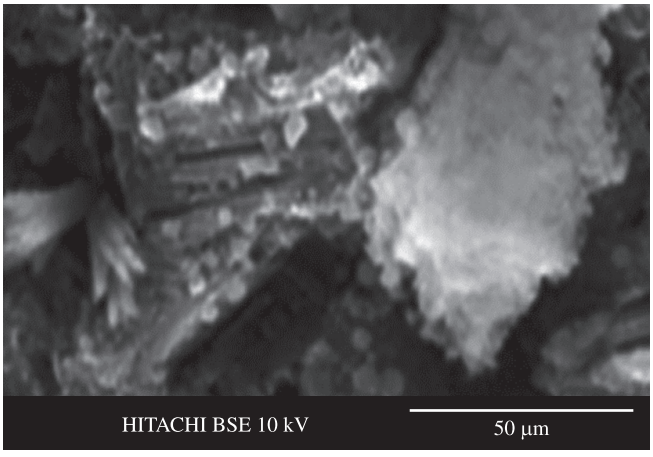

Figure 3. SEM micrograph of cement paste with ZnO_2 nanoparticles cured in water.

2. The difference between compressive strengths of the N-W and N-LW series after 28 days of curing is relatively high while this difference in compressive strength after 90 days of curing is not high. This may be due to formation of crystalline $Ca(OH)_2$ in N-LW series after the 28 day causes reduction in compressive strength. In the other words, curing of the ZnO_2 nanoparticles blended concrete in saturated limewater after 28 days is completely suitable to achieve high strength especially with high weight percent of nanoparticles.

Figures 5 and 6 show the SEM micrograph of concrete without and with ZnO_2 nanoparticles at 7 days of curing in saturated limewater. Once again, the micrograph of the mixture containing nano- ZnO_2 revealed a compact formation of hydration products and a reduced content of $Ca(OH)_2$ crystals. Moreover, No significant differences is evident between the microstructure of concrete without nano- ZnO_2 cured in water or saturated limewater. In addition XRD results of the cement pastes with ZnO_2 nanoparticles at 15 hours of curing in saturated limewater have been illustrated in Figure 4. The longer pick intensity show that the amount of $Ca(OH)_2$ crystals which needs to formation of C-S-H gel is more for the specimens cured in limewater rather the specimens cured in water when ZnO_2 nanoparticles are used.

3.2. Split tensile strength and flexural strength

The split tensile strength and flexural strength results of C0 and N series mixtures are shown in Figures 7 and 8, respectively. The results again shows the better tensile strength in ZnO_2 nanoparticles blended concrete with respect to the control concrete specially in high volume fraction of nanoparticles in concrete cured at saturated limewater. This again may be due to more C-S-H gel formation in the presence of nanoparticles especially for the specimens cured at saturated limewater after 28 days of curing.

Since evaluations of strength with different tests are not affordable, here, the relationship between compressive strength and split tensile strength, and the relationship between compressive strength and flexural strength is presented. Figure 9a, b and c show the relationship between the splitting tensile strength and compressive strength of all mixes cured for 2, 7 and 28 days, respectively. In addition, Figure 10a, b and c show the relationship between the flexural strength and compressive strength of all mixes cured for 2, 7 and 28 days, respectively. In all curves, a logarithmic relation has been adopted to show this relationship. The R-squared values are also given in the figures and show a good compatibility between two specified strength. As figures show, at every age of curing, one may predict a specified strength by knowing at least one of the specimens' strength.

3.3. Percentage of water absorption

The results of saturated water absorption at different ages of moist curing are shown in Figure 11. As it can be seen, the percentage of water absorption of concrete samples immersed in water and saturated limewater decreases with the increase in the age of moist curing from 7 to 90 days for all series during the hardening process of the concrete. In the other words, C-S-H gel formation in the presence of nanoparticles especially for the specimens cured at saturated limewater are high enough reduces the water absorption of the blended concrete. This reduction is more for N-LW series as a result of more C-S-H gel formation. However this difference is not too high because of this fact that the water permeability is significantly related to the content of pores in the concrete which is equal for two N-W and N-LW series at a certain nanoparticle content.

It was observed that the reduction of water absorption was found at the 7 days curing for N series compared to C0 series. The decrease in water absorption which is related to the increase in the amount

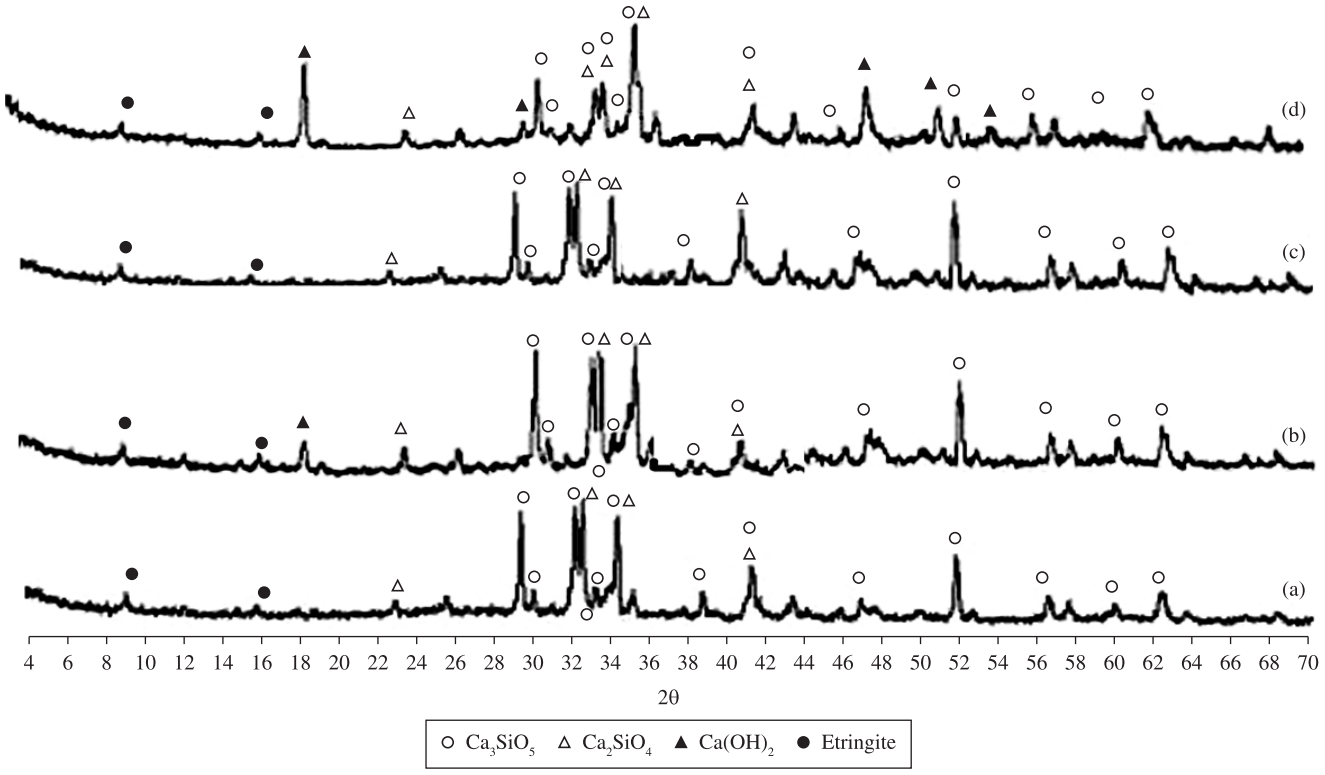

Figure 4. XRD results of cement pastes at 15 hours of curing for specimens a) without ZnO_2 nanoparticles cured in water; b) with ZnO_2 nanoparticles cured in water; c) without ZnO_2 nanoparticles cured in saturated limewater; and d) with ZnO_2 nanoparticles cured in saturated limewater.

of ZnO_2 nanoparticles can be resulted from the reduced amount of pores. These results were achieved because of fewer hydration products when the pozzolanic reaction is small at the early ages for C0 series reverse of the N series. On the other hand, the percentage of water absorption related to the porosity of the hardened concrete which is engaged by water in saturated state[50] was more in C0 series compared to N series at the early ages. But by increasing the age of curing to 90 days the percentage of water absorption values decreases significantly with the increase in nanoparticles content up to 2.0%. Therefore, it can be suggested that with prolonged curing, increasing the ages and percentages of ZnO_2 nanoparticles in both series can lead to reduction in permeable voids. This is due to the pozzolanic action of ZnO_2 nanoparticles and filler effect provided by both series of ZnO_2 nanoparticles. Another finding is that the interfacial transition zone in concrete had improved due to pozzolanic reaction as well as filler effect of the ZnO_2 nanoparticles.

3.4. Workability

A high-quality concrete is one which has acceptable workability (around 6.5 cm slump height) in the fresh condition and develops sufficient strength. Basically, the bigger the measured height of slump, the better the workability will be, indicating that the concrete flows easily but at the same time is free from segregation[51,52]. Maximum strength of concrete is related to the workability and can only be obtained if the concrete has adequate degree of workability because of self compacting ability. Self-compacting repair mortars, as new technology products, are especially preferred for the rehabilitation and repair of reinforced concrete structures[53]. The water/powder (cement, fly ash, limestone filler, silica fume, nanoparticles, etc.) ratio of mortar and the type of chemical admixtures should be determined, in order to place the fresh mortar without any external compaction and at the same time without causing any segregation[54]. In other words, the rheology of paste phase of self-repairing mortar should have suitable properties from flowability and segregation point of view[55-58].

The workability of C0 and N series concrete are presented in Figure 12. The figure shows the influence of ZnO_2 nanoparticles content on the workability of mixtures at constant water to binder ratio of 0.40. The results show that unlike the C0 series, all investigated nano- ZnO_2 nanoparticles blended mixtures had low slump values and non-acceptable workability. This may be due to the increasing in the surface area of powder after adding nanoparticles that needs more water to wetting the cement nanoparticles. The reduction in workability in N-LW series is higher than that of N-W series because of more rapid formation of C-S-H gel results in a more viscose mortar with reduced workability.

With the improvement of novel plasticizers, to obtain high filling rates is possible even for compound molding systems. The fresh characteristics of concrete, strength and durability of mortars can be improved by the addition of inert or pozzolanic[59]. The selection of the amount and the type of cementitious or inert powders depends on the physical and physico-chemical properties of these powders which are affecting the performance of fresh paste such as nanoparticle shape, surface texture, surface porosity and rate of superplasticizer adsorption, surface energy (zeta potential), finest fraction content, Blaine fineness and nanoparticle size distribution.

There is no universally accepted agreement on the effect of these factors due to the complex influence of the combination of these factors[60].

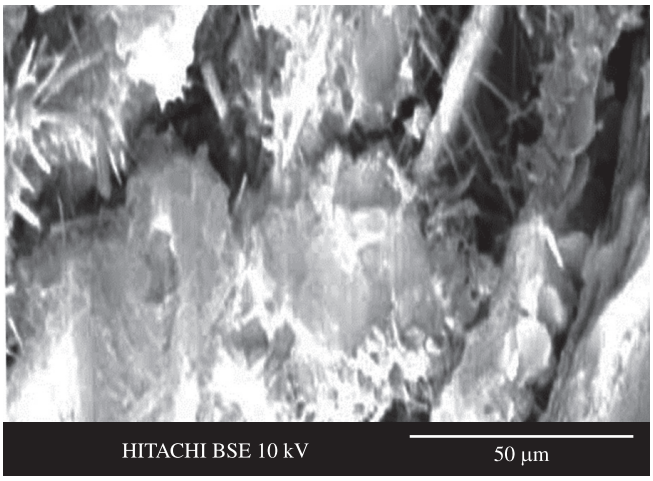

Figure 5. SEM micrograph of cement paste without ZnO_2 nanoparticles cured in saturated limewater.

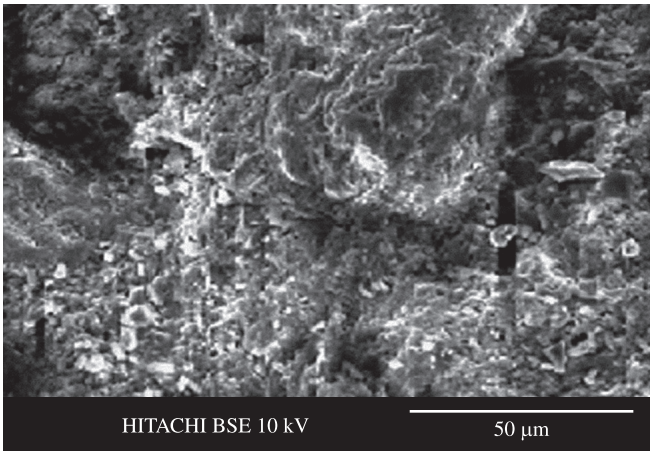

Figure 6. SEM micrograph of cement paste with ZnO_2 nanoparticles cured in saturated limewater.

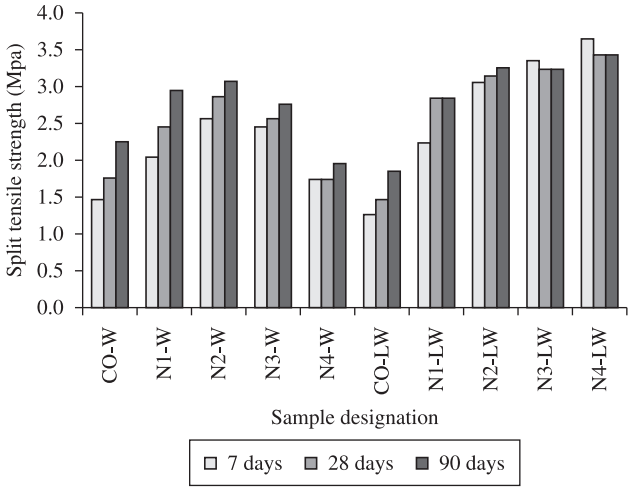

Figure 7. Split tensile strength of nano- ZnO_2 particle blended concrete specimens.

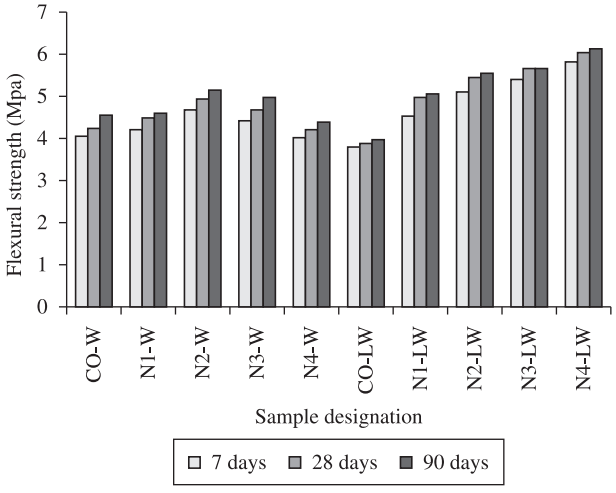

Figure 8. Flexural strength of nano- ZnO_2 particle blended concrete specimens.

Usually, increasing the fine nanoparticles content in cements changes the rheological properties of pastes and consequently influences the workability of mortars and fresh concrete mixtures. The observed changes can be advantageous or not as a result of many factors influencing the rheology of cement pastes[61]. It is usually expected that, if the volume concentration of a solid is held constant, for a specific workability, the replacement of cement with a fine powder will increase the water demand due to the increase in surface area. This is more observed for nanoparticles blended concrete. However, in some cases, the above-mentioned conclusion is not appropriate. Lange et al.[62] obtained same results with fly ash blended concrete. But In this study, the addition of nano- ZnO_2 nanoparticles decreased the fluidity and increased the water demand for normal consistency

3.5. Pore structure of concrete

The pore structure of concrete is the general embodiment of porosity, pore size distribution, pore scale and pore geometry. The test results of MIP in this study include the pore structure parameters such as total specific pore volume, most probable pore diameter, pore size distribution, porosity, average diameter, and median diameter (volume).

In terms of the different effect of pore size on concrete performance, the pore in concrete is classified as harmless pore (<20 nm), few-harm pore (20~50 nm), harmful pore (50~200 nm) and multi-harm pore (>200 nm)[63]. In order to analyze and compare conveniently, the pore structure of concrete is divided into four ranges according to this sort method in this work.

3.5.1. Total specific pore volume and most probable pore diameter of concrete

Table 4 shows that with the addition of ZnO_2 nanoparticles, the total specific pore volumes of concretes is decreased, and the most probable pore diameters of concretes shift to smaller pores and fall in the range of few-harm pore, which indicates that the addition of nanoparticles refines the pore structure of concretes.

The effectiveness of nano- ZnO_2 in reducing the total specific pore volumes and most probable pore diameters of concretes increases in the order N4-W<N1-W<N3-W<N2-W series for the specimens cured in water and N1-LW<N2-LW<N3-LW<N4-LW for the specimens cured in saturated limewater.

With increasing the content of nanoparticles, the reduced extent of total specific pore volume and most probable pore diameter increases, and the refinement on the pore structure of concretes is improved.

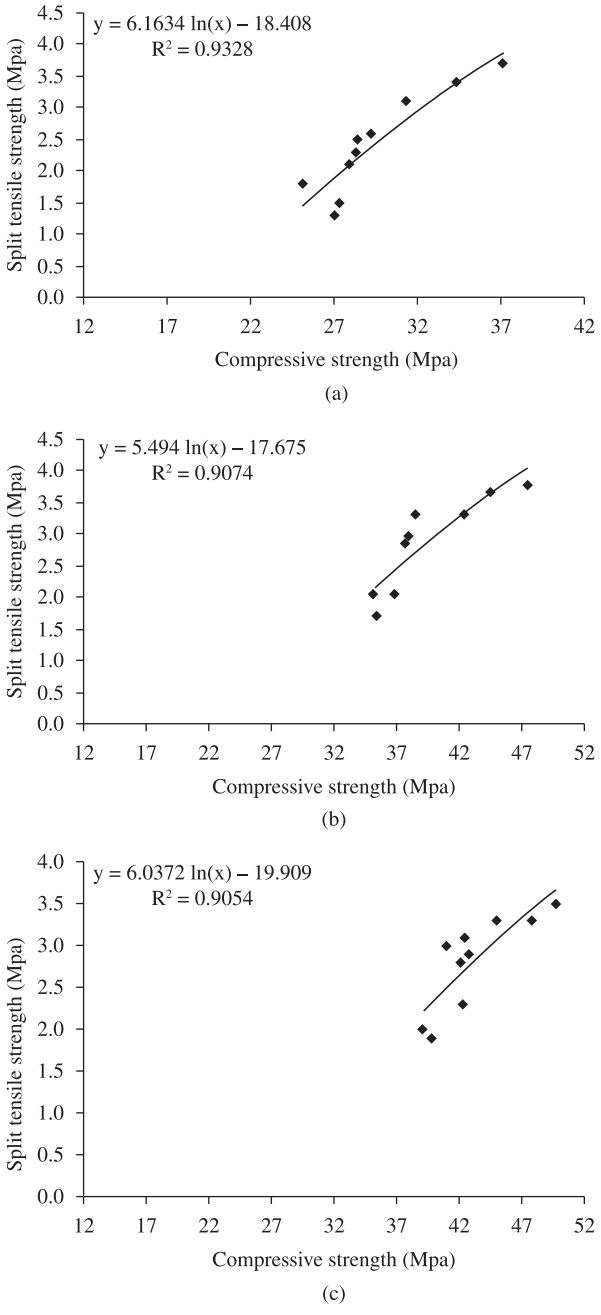

Figure 9. The relationship between split tensile strength and compressive strength of the specimens cured at a) 7 days; b) 28 days; and c) 90 days.

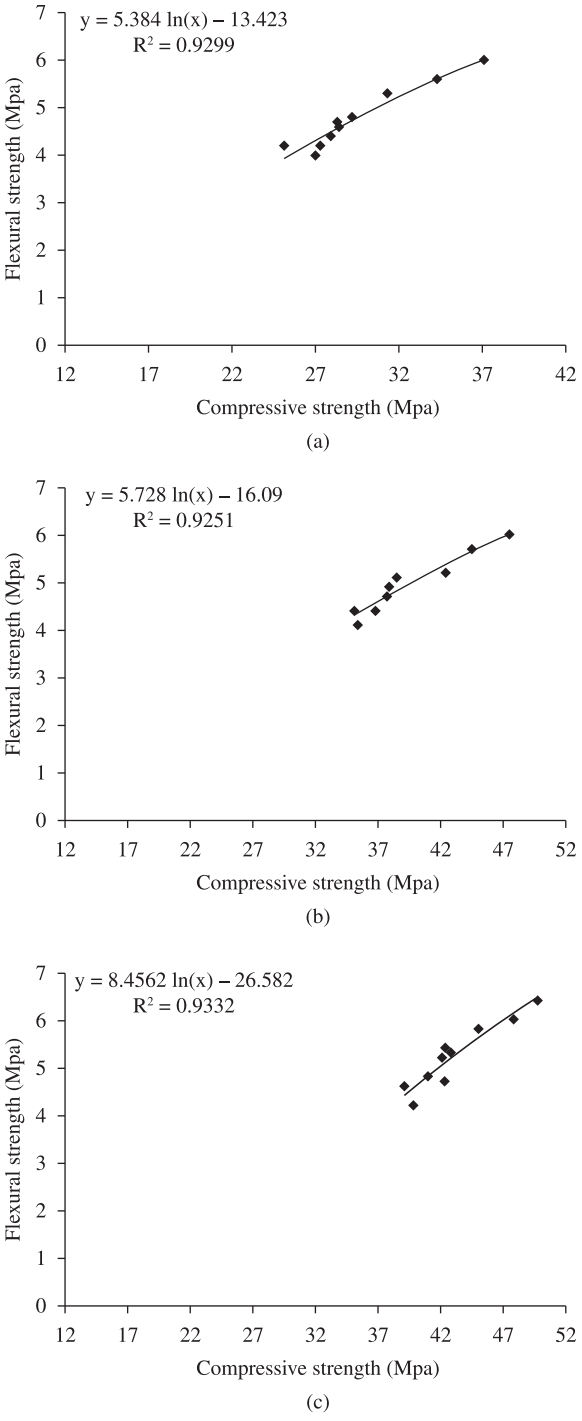

Figure 10. The relationship between flexural strength and compressive strength of the specimens cured at a) 7 days; b) 28 days; and c) 90 days.

Table 5 gives the porosities, average diameters and median diameters (volume) of various concretes. The regularity of porosity is similar to that of total specific pore volume. The regularity of average diameter and median diameter (volume) is similar to that of most probable pore diameter. Therefore, it is no longer necessary to analyze one by one herein.

3.5.2. Pore size distribution of concrete

The pore size distribution of concretes is shown in Table 6. It can be seen that by the addition of nano-particles, the amounts of pores decrease, which shows that the density of concretes is increased and the pore structure is improved.

The effectiveness of nano-SiO_2 in improving the pore structure of concretes increases in the order N4-W<N1-W<N3-W<N2-W series for the specimens cured in water and N1-LW<N2-LW<N3-LW<N4-LW for the specimens cured in saturated limewater.

The harmless and few-harm pores in N2-W and N4-LW series increase by the largest extent, while its harmful and multi-harm pores decrease by the largest extent, which indicates that the pore structure of N2-W and N4-LW series is most significantly improved. With increasing of nanoparticles' content, the extent pores in concretes

are all decreased, and the improvement on the pore structure of concretes is evident.

The mechanism that the nanoparticles improve the pore structure of concrete can be interpreted as follows. Supposed that nanoparticles are uniformly dispersed in concrete and each particle is contained in a cube pattern, the distance between nanoparticles can be determined. After hydration begins, hydrate products diffuse and envelop nanoparticles as kernel. If the content of nanoparticles and the distance between them are appropriate, the crystallization will be controlled to be a suitable state through restricting the growth of $Ca(OH)_2$ crystal by nanoparticles. Moreover, the nanoparticles located in cement paste as kernel can further promote cement hydration due to their

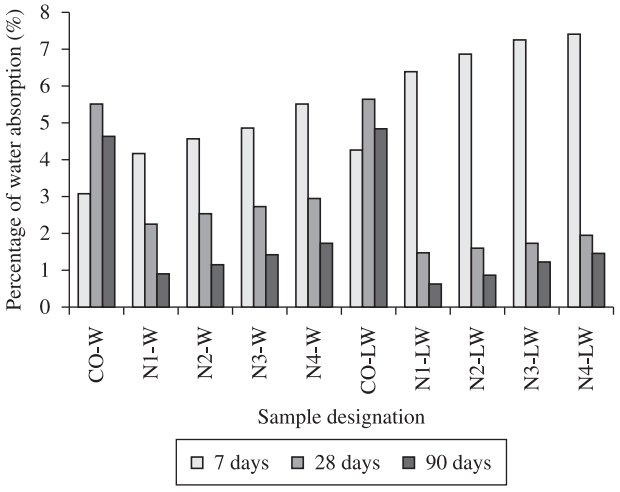

Figure 11. Percentage of water absorption of nano-ZnO_2 particle blended concrete specimens.

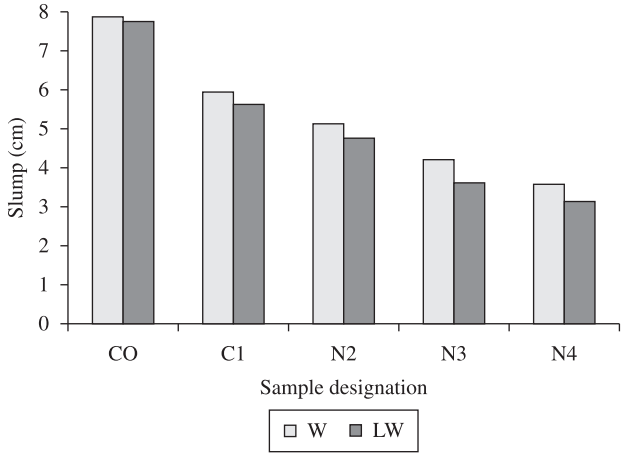

Figure 12. Workability of concrete containing ZnO_2 nanoparticles. N1, N2, N3 and N4 are the series N blended concrete with 0.5, 1.0, 1.5 and 2.0% of ZnO_2 nanoparticles, respectively. W denotes the specimens cured in water and LW denotes to those cured in saturated limewater.

Table 4. Total specific pore volumes and most probable pore diameters of concretes.

Mixture	Total specific pore volume		Most probable pore diameter	
Type	Value ($mL.g^{-1}$)	Reduced extent (%)	Value ($mL.g^{-1}$)	Reduced extent (%)
C0-W (control)	0.0481	0	42	0
N1-W	0.0454	+5.42	35	+17.42
N2-W	0.0460	+4.70	36	+18.52
N3-W	0.0464	+3.74	37	+15.08
N4-W	0.0469	+2.59	40	+6.16
C0-LW (control)	0.0466	0	40	0
N1-LW	0.0434	+6.75	31	+23.50
N2-LW	0.0439	+6.19	32	+27.93
N3-LW	0.0445	+4.70	35	+17.16
N4-LW	0.0450	+3.46	37	+9.64

Water to binder [cement + nano- ZnO_2] ratio of 0.40; W denotes the specimens cured in water and LW denotes to those cured in saturated limewater.

Table 5. Prosities, average diameters and median diameters (volume) of concretes.

Mixture	Prosity		Average diameter		Median diameter (volume)	
Type	Value (%)	Reduced extent (%)	Value (nm)	Reduced extent (%)	Value (nm)	Reduced extent (%)
C0-W (control)	9.99	0	37.53	0	51.40	0
N1-W	9.19	+8.00	32.53	+13.30	43.35	+15.66
N2-W	9.40	+5.59	34.68	+8.93	45.69	+13.42
N3-W	9.64	+3.66	36.31	+3.58	48.85	+5.67
N4-W	9.75	+2.52	37.84	-0.87	51.40	-0.01
C0-LW (control)	9.66	0	34.20	0	48.70	0
N1-LW	8.36	+16.83	30.70	+19.96	40.90	+21.55
N2-LW	8.58	-4.73	32.94	-9.45	43.24	-7.85
N3-LW	8.87	+13.25	33.66	+11.98	45.18	+14.65
N4-LW	9.07	-4.34	36.10	-9.41	48.85	-10.28

Water to binder [cement + nano- ZnO_2] ratio of 0.40; W denotes the specimens cured in water and LW denotes to those cured in saturated limewater.

high activity. This makes the cement matrix more homogeneous and compact. Consequently, the pore structure of concrete is improved evidently such as the concrete containing nano- ZnO_2 in the amount of 2.0% by weight of nanoparticles.

With increasing content of nanoparticles, the improvement on the pore structure of concrete is evident. This can be attributed to that the distance between nanoparticles decreases with increasing content of nanoparticles, and $Ca(OH)_2$ crystal cannot grow up enough due to limited space and the crystal quantity is decreased, which leads to the ratio of crystal to strengthening gel small and the shrinkage and creep of cement matrix is decreased[63], thus the pore structure of cement matrix is better relatively.

On the whole, the addition of nanoparticles improves the pore structure of concrete. On the one hand, nanoparticles can act as a filler to enhance the density of concrete, which leads to the porosity of concrete reduced significantly. On the other hand, nanoparticles can not only act as an activator to accelerate cement hydration due to their high activity, but also act as a kernel in cement paste which makes the size of $Ca(OH)_2$ crystal smaller and the tropism more stochastic.

3.6. Conduction calorimetry

Two signals can be distinguished on all test results: a peak corresponding to the acceleration or post-induction period, associated with the precipitation of C–S–H gel and CH, and a shoulder related to a second, weaker signal with a later peak time, associated with the transformation from the ettringite (AFt) to the calcium monosulphoaluminate (AFm) phase via dissolution and reaction with $Al(OH)^{4-}$[64]. The numerical values corresponding to these two signals (heat release rate, peak times) and the total released heat are shown in Table 7. The time period over the total heat was measured until the heat release rate was below 1% of the maximum of the second peak.

The heat release rate values in Table 7 show that decreasing the percentage of nanoparticles in the pastes retards peak times and raises heat release rate values. In addition, the specimens which have been cured in saturated limewater show a decreased peak time and heat release rate values with respect to the corresponding specimens cured in water. This is indicative of a delay in initial cement hydration due to lesser content of nanoparticles and the lesser content of $Ca(OH)_2$ in the specimens cured in water. The retardation is much less marked in the second peak. The total heat released under identical conditions (at times when the heat release rate is less than 1% of the maximum amount of heat released in the first peak) decreases with higher percentages of ZnO_2 nanoparticles in the mix.

3.7. Thermogravimetric analysis results

Table 8 shows the weight loss measured in the 110-650 °C range in which dehydration of the hydrated products occurred. The results show that after 90 days of curing, the loss in weight of the specimens is increased by increasing the nanoparticles content in concretes. This is more evident in N2-W and N4-LW series. This

Table 6. Pore size distribution of concretes.

Mixture	Pore size distribution ($mL.g^{-1}$(%))				Total specific pore volume ($mL.g^{-1}$)
Type	Harmless pores (<20 nm)	Few-harm pores (20~50 nm)	Harmful pores (50~200 nm)	Multi-harm pores (>200 nm)	
C0-W (control)	0.0065	0.0147	0.0169	0.0099	0.0481
N1-W	0.0067	0.0169	0.0143	0.0077	0.0454
N2-W	0.0068	0.0164	0.0150	0.0081	0.0460
N3-W	0.0069	0.0159	0.0157	0.0086	0.0464
N4-W	0.0069	0.0154	0.0161	0.0090	0.0469
C0-LW (control)	0.0067	0.0157	0.0148	0.0091	0.0466
N1-LW	0.0070	0.0178	0.0124	0.0065	0.0434
N2-LW	0.0070	0.0173	0.0130	0.0069	0.0439
N3-LW	0.0070	0.0169	0.0142	0.0072	0.0445
N4-LW	0.0071	0.0163	0.0144	0.0076	0.0450

Water to binder [cement + nano- ZnO_2] ratio of 0.40; W denotes the specimens cured in water and LW denotes to those cured in saturated limewater.

Table 7. Calorimetric results of cement pastes.

Mixture	Total heat	First peak		Second peak	
	$kJ.kg^{-1}$	Time (hour)	Rate ($W.kg^{-1}$)	Time (hour)	Rate ($W.kg^{-1}$)
C0-W (control)	299.8	1.4	0.6	15.1	2.5
N1-W	254.4	1.1	0.5	13	2.2
N2-W	233.2	1	0.5	11.5	2
N3-W	256.3	1.1	0.6	13.2	2.2
N4-W	281.9	1.3	0.6	14.2	2.3
C0-LW (control)	312.5	1.6	0.6	15.8	2.6
N1-LW	238.7	1.5	0.6	14.3	2.3
N2-LW	246.6	1.4	0.6	11.8	2
N3-LW	233.1	1.2	0.5	10.2	2
N4-LW	212.5	0.9	0.5	8.8	1.9

Water to binder [cement + nano- ZnO_2] ratio of 0.40; W denotes the specimens cured in water and LW denotes to those cured in saturated limewater.

Table 8. Weight loss (%) of the pastes in the range of 110-650 °C after 90 days of curing.

Mixture	Total heat
	$kJ.kg^{-1}$
C0-W (control)	12.2
N1-W	11.5
N2-W	11.7
N3-W	11.6
N4-W	11.4
C0-LW (control)	12.7
N1-LW	12.1
N2-LW	11.8
N3-LW	11.4
N4-LW	11.1

Water to binder [cement + nano- ZnO_2] ratio of 0.40; W denotes the specimens cured in water and LW denotes to those cured in saturated limewater.

may be due to more formation of hydrated C-S-H gel in N2-W and N4-LW series.

4. Conclusions

The results show that the specimens containing ZnO_2 nanoparticles have significantly higher strength with comparison to that of specimens without nano- ZnO_2 particles at every age of curing. It is found that the cement could be advantageously replaced with nano- ZnO_2 particles up to maximum limit of 2.0% with average particle sizes of 15 nm when the specimens cured at saturated limewater. The optimum level of nano- ZnO_2 particles content was achieved 1.0% for the specimens cured in water. Partial replacement of cement by nano- ZnO_2 particles decreased percentage of water absorption of concrete specimens. However, the workability of concrete was reduced by adding ZnO_2 nanoparticles and hence plasticizers were added to improve the workability of the specimens. ZnO_2 nanoparticles could accelerate the appearance of the first peak in conduction calorimetry test which is related to the acceleration in formation of hydrated cement products. Thermogravimetric analysis shows that ZnO_2 nanoparticles could increase the weight loss of the specimens when partially added to cement paste. More rapid formation of hydrated products could in presence of ZnO_2 nanoparticles which was confirmed by XRD results could be the reason of more weight loss. The pore structure of self compacting concrete containing ZnO_2 nanoparticles is improved and the content of all mesopores and macropores is increased.

References

1. Li H, Xiao HG, Yuan J and Ou J. Microstructure of cement mortar with nano-particles. *Composites Part B*: Engineering. 2004; 35:185-189. doi:10.1016/S1359-8368(03)00052-0
2. Ji T. Preliminary study on the water permeability and microstructure of concrete incorporating nano-SiO_2. *Cement and Concrete Research*. 2005; 35(10):1943-1947. doi:10.1016/j.cemconres.2005.07.004
3. Jo B-W, Kim C-H, Tae G-H and Park J-B. Characteristics of cement mortar with nano-SiO_2 particles. *Construction and Building Materials*. 2007; 21(6):1351-1355. doi:10.1016/j.conbuildmat.2005.12.020
4. Li H, Xiao H-G and Ou J-P. A study on mechanical and pressure-sensitive properties of cement mortar with nanophase materials. *Cement and Concrete Research*. 2004; 34(3):435-438. doi:10.1016/j.cemconres.2003.08.025
5. Li H, Zhang M-H and Ou J-P. Abrasion resistance of concrete containing nanoparticles for pavement. *Wear* 2006; 260(11-12):1262-1266. doi:10.1016/j.wear.2005.08.006
6. Qing Y, Zenan Z, Deyu K and Rongshen C. Influence of nano-SiO_2 addition on properties of hardened cement paste as compared with silica fume. *Construction and Building Materials*. 2007; 21(3):539-545. doi:10.1016/j.conbuildmat.2005.09.001
7. Lin KL, Chang WC, Lin DF, Luo HL and Tsai MC. Effects of nano-SiO_2 and different ash particle sizes on sludge ash-cement mortar. *Journal of Environmental Management*. 2008; 88(4):708-714. PMid:17498863. doi:10.1016/j.jenvman.2007.03.036
8. Lin DF, Lin KL, Chang WC, Luo HL and Cai MQ. Improvements of nano-SiO_2 on sludge/fly ash mortar. *Waste Management*. 2008; 28(6):1081-1087. PMid:17512717. doi:10.1016/j.wasman.2007.03.023
9. Sobolev K, Flores I, Torres-Martinez LM, Valdez PL, Zarazua E and Cuellar EL. Engineering of SiO_2 nanoparticles for optimal performance in nano cementbased materials. In: Bittnar Z, Bartos PJM, Nemecek J, Smilauer V and Zeman J, editors. *Nanotechnology in construction*: proceedings of the NICOM3 (3th International Symposium on Nanotechnology in Construction). Prague: Springer; 2009. p. 139-148.
10. Qing Y, Zenan Z, Li S and Rongshen C. A comparative study on the pozzolanic activity between nano-SiO_2 and silica fume. *Journal of Wuhan University of Technology* - Materials Science Education. 2008; 21(3):153-157.
11. Sobolev K and Ferrada-Gutiérrez M. How nanotechnology can change the concrete world: part 2. *American Ceramic Society Bulletin*. 2005; 84(11):16-19.
12. Li H, Zhang M-H and Ou J-P. Flexural fatigue performance of concrete containing nano-particles for pavement. *International Journal of Fatigue*. 2007; 29(7):1292-1301. doi:10.1016/j.ijfatigue.2006.10.004
13. Li Z, Wang H, He S, Lu Y and Wang M. Investigations on the preparation and mechanical properties of the nano-alumina reinforced cement composite. *Materials Letter*. 2006; 60(3):356-359. doi:10.1016/j.matlet.2005.08.061
14. Garboczi EJ and Bentz DP. Modelling of the microstructure and transport properties of concrete. *Construction and Building Materials*. 1996; 10(5):293-300. doi:10.1016/0950-0618(94)00019-0
15. Chang T-P, Shih J-Y, Yang K-M and Hsiao T-C. Material properties of Portland cement paste with nano-montmorillonite. *Journal of Materials Science*. 2007; 42(17):7478-7487. doi:10.1007/s10853-006-1462-0
16. Kuo W-Y, Huang J-S and Lin C-H. Effects of organo-modified montmorillonite on strengths and permeability of cement mortars. *Cement and Concrete Research*. 2006; 36(5):886-895. doi:10.1016/j.cemconres.2005.11.013
17. Lee SJ and Kriven WM. Synthesis and hydration study of Portland cement components prepared by the organic steric entrapment method. *Materials & Structures*. 2005; 38(1):87-92. doi:10.1007/BF02480579
18. Nazari A and Riahi S. Microstructural, thermal, physical and mechanical behavior of the self compacting concrete containing SiO_2 nanoparticles. *Materials Science and Engineering*: A. 2010; 527:7663-7672. doi:10.1016/j.msea.2010.08.095
19. Nazari A and Riahi S. The effects of SiO_2 nanoparticles on physical and mechanical properties of high strength compacting concrete. *Composites Part B*: Engineering. 2011; 42(3):570-578. doi:10.1016/j.compositesb.2010.09.025
20. Nazari A and Riahi S. The role of SiO_2 nanoparticles and ground granulated blast furnace slag admixtures on physical, thermal and mechanical properties of self compacting concrete. *Materials Science and Engineering:* A. 2011; 528(4-5): 2149-2157. doi:10.1016/j.msea.2010.11.064
21. Nazari A and Riahi S. Splitting tensile strength of concrete using ground granulated blast furnace slag and SiO_2 nanoparticles as binder. *Energy and Buildings*. 2011; 43(4):864-872. doi:10.1016/j.enbuild.2010.12.006
22. Nazari A and Riahi S. The effect of TiO_2 nanoparticles on water permeability and thermal and mechanical properties of high strength self-compacting concrete. *Materials Science and Engineering*: A. 2010; 528(2):756-763. doi:10.1016/j.msea.2010.09.074
23. Nazari A. The effects of curing medium on flexural strength and water permeability of concrete incorporating TiO_2 nanoparticles. *Materials & Structures*. 2011; 44(4):773-786. doi:10.1617/s11527-010-9664-y
24. Nazari A and Riahi S. The effects of TiO_2 nanoparticles on physical, thermal and mechanical properties of concrete using ground granulated

blast furnace slag as binder. *Materials Science and Engineering*: A. 2011; 528(4-5):2085-2092. doi:10.1016/j.msea.2010.11.070

25. Nazari A and Riahi S. TiO_2 nanoparticles effects on physical, thermal and mechanical properties of self compacting concrete with ground granulated blast furnace slag as binder. *Energy and Buildings*. 2010; 43(4):995-1002.
26. Nazari A and Riahi S. Improvement compressive strength of concrete in different curing media by Al_2O_3 nanoparticles. *Materials Science and Engineering*: A. 2011; 528(3):1183-1191. doi:10.1016/j.msea.2010.09.098
27. Nazari A and Riahi S. Al_2O_3 nanoparticles in concrete and different curing media. *Energy and Buildings*. 2011; 43(6):1480-1488. doi:10.1016/j.enbuild.2011.02.018
28. Nazari A and Riahi S. The effects of zinc dioxide nanoparticles on flexural strength of self-compacting concrete. *Composites Part B*: Engineering. 2011; 42(2):167-175. doi:10.1016/j.compositesb.2010.09.001
29. Nazari A and Riahi S. ZrO_2 nanoparticles' effects on split tensile strength of self compacting concrete. *Materials Research*. 2010; 13(4):485-495. doi:10.1590/S1516-14392010000400011
30. Nazari A and Riahi S. The Effects of ZrO_2 Nanoparticles on Physical and Mechanical Properties of High Strength Self Compacting Concrete. *Materials Research*. 2010; 13(4):551-556. doi:10.1590/S1516-14392010000400019
31. Nazari A and Riahi S. Limewater effects on properties of ZrO_2 nanoparticle blended cementitious composite. *Journal of Composite Materials*. 2011; 45(6):639-644. doi:10.1177/0021998310376118
32. Nazari A and Riahi S. Assessment of the effects of Fe_2O_3 nanoparticles on water permeability, workability, and setting time of concrete. *Journal of Composite Materials*. 2011; 45(8):923-930. doi:10.1177/0021998310377945
33. Nazari A and Riahi S. The effects of Cr_2O_3 nanoparticles on strength assessments and water permeability of concrete in different curing media. *Materials Science and Engineering*: A. 2011; 528(3):1173-1182. doi:10.1016/j.msea.2010.09.099
34. Nazari A and Riahi S. Optimization mechanical properties of Cr_2O_3 nanoparticle binary blended cementitious composite. *Journal of Composite Materials*. 2011; 45(8):943-948. doi:10.1177/0021998310377944
35. Nazari A and Riahi S. Effects of CuO Nanoparticles on Microstructure, Physical, Mechanical and Thermal Properties of Self-Compacting Cementitious Composites. *Journal of Materials Science & Technology*. 2011; 27(1):81-92.
36. Sobolev K and Ferrada-Gutiérrez M. How nanotechnology can change the concrete world: Part 1. *American Ceramic Society Bulletin*. 2005; 10:14-17.
37. Sobolev K and Ferrada-Gutiérrez M. How nanotechnology can change the concrete world: Part 2. *American Ceramic Society Bulletin*. 2005; 11:16-19.
38. Perraton D, Aïtcin PC and Carles-Gbergues A. Permeability, as seen by the researcher. In: Malier Y, editor. *High Performance Concrete*: from material to structure. London: E & FN Spon; 1994. p.186-195.
39. Ye G, Lura P and van Breugel K. Modelling of water permeability in cementitious materials. *Materials and Structures*. 2006; 39:877-885. doi:10.1617/s11527-006-9138-4
40. American Society for Testing and Materials. *ASTM C150, Standard Specification for Portland Cement, annual book of ASTM standards*. Philadelphia: ASTM; 2001.
41. American Society for Testing and Materials. *ASTM C39, Standard Test Method for Compressive Strength of Cylindrical Concrete Specimens*. Philadelphia: ASTM; 2001.
42. American Society for Testing and Materials. *ASTM C496, Standard Test Method for Splitting Tensile Strength of Cylindrical Concrete Specimens*. Philadelphia: ASTM; 2001.
43. American Society for Testing and Materials. *ASTM C293, Standard Test Method for Flexural Strength of Concrete (Using Simple Beam with Center-Point Loading)*. Philadelphia: ASTM; 2001.
44. American Society for Testing and Materials. *ASTM C143, Standard Test Method for Slump of Hydraulic-Cement Concrete*. Philadelphia: ASTM; 2001.
45. American Society for Testing and Materials. *ASTM C642, Standard Test Method for Density, Absorption, and Voids in Hardened Concrete.* Philadelphia: ASTM; 2001.
46. Abell AB, Willis KL and Lange DA. Mercury Intrusion Porosimetry and Image nalysis of Cement-Based Materials. *Journal of Colloid and Interface Science*. 1999; 211:39-44. PMid:9929433. doi:10.1006/jcis.1998.5986
47. Tanaka K and Kurumisawa K. Development of technique for observing pores in hardened cement paste. *Cement and Concrete Research*. 2002; 32:1435-1441. doi:10.1016/S0008-8846(02)00806-2
48. Hall C. Water sorptivity of mortars and concretes: a review. *Magazine of Concrete Research*. 1989; 41(14):51-61. doi:10.1680/macr.1989.41.147.51
49. Mostafa NY and Brown PW. Heat of hydration of high reactive pozzolans in blended cements: Isothermal conduction calorimetry. *Thermochimica Acta.* 2005; 435:162-167. doi:10.1016/j.tca.2005.05.014
50. AI-Khalaf MN and Yousift HA. Use of rice husk ash in concrete. *International Journal of Cement Composites and Lightweight Concrete*. 1984; 6(4):241-248.
51. Lin YH, Tyan YY, Chang TP and Chang CY. An assessment of optimal mixture for concrete made with recycled concrete aggregates. *Cement and Concrete Research*. 2004; 34(8):1373-1380. doi:10.1016/j.cemconres.2003.12.032
52. Tattersall GH and Baker PH. An instigation of the effect of vibration on the workability of fresh concrete using a vertical pipe apparatus. *Magazine of Concrete Research*. 1989; 14(146):3-9. doi:10.1680/macr.1989.41.146.3
53. Courard L, Darimont A, Willem X, Geers C and Degeimbre R. Repairing concretes with self-compacting concrete: testing methodology assessment. In: *Proceedings of the First North American Conference on the Design and Use of Self-Consolidating Concrete*; 2002; Chicago. Chicago; 2002. p. 267-274.
54. Felekoglu B, Tosun K, Baradan B, Altun A and Uyulgan B. The effect of fly ash and limestone fillers on the viscosity and compressive strength of self-compacting repair mortars. *Cement and Concrete Research*. 2008; 36:1719-1726. doi:10.1016/j.cemconres.2006.04.002
55. Banfill PFG. The Rheology of Fresh Cement and Concrete-A Review. In: *Proceedings of the 11th International Cement Chemistry Congress;* 2003; Durban. Durban: PCA; 2003. p. 50-62
56. Lemmer C, Hartman J and Wolf T. *Rheological properties of mortars for self-compacting concrete*. 13 p. Available from: <http://www.massivbau.tu-darmstadt.de/user/lemmer/web/scc/LeDaCon199.htm>.
57. Ferraris CF and Gaidis JM. Connection between the rheology of concrete and rheology of cement paste. *ACI Materials Journal*. 1992; 89(4):388-393.
58. Ferraris CF. Measurement of the rheological properties of high performance concrete: state of the art report. *Journal National Institute of Standards and Technology*. 1999; 104:461-478.
59. Cyr M, Legrand C and Mouret M. Study of the shear thickening effect of superplasticizers on the rheological behavior of cement paste containing or not mineral admixtures. *Cement and Concrete Research*. 2000; 30:1477-1483. doi:10.1016/S0008-8846(00)00330-6
60. Ferraris CF, Obla KH and Hill R. The influence of mineral admixtures on the rheology of cement paste and concrete. *Cement and Concrete Research*. 2001; 31:245-255. doi:10.1016/S0008-8846(00)00454-3
61. Grzeszczyk S and Lipowski G. Effect of content and nanoparticle size distribution of high-calcium fly ash on the rheological properties of cement pastes. *Cement and Concrete Research*. 1997; 27:907-916. doi:10.1016/S0008-8846(97)00073-2
62. Lange F, Mortel N and Rudert V. Dense packing of cement pastes and resulting consequences on mortar properties. *Cement and Concrete Research*. 1997; 27:1481-1488. doi:10.1016/S0008-8846(97)00189-0
63. Ye Q. The study and development of the nano-composite cement structure materials. *New building Materials.* 2001; (1):4-6.
64. Jawed J, Skalny J and Young JF. *Hydration of Portland Cement*: Structure and Performance of Cements. Essex: Applied Science Publishers; 1983. p. 284-285.